In situ oxygen incorporation and related issues in CdTe/CdS photovoltaic devices

M. Emziane,[a] K. Durose, and D. P. Halliday
Department of Physics, University of Durham, South Road, Durham, DH1 3LE, United Kingdom

A. Bosio and N. Romeo
Department of Physics, University of Parma, Parco Area delle Scienze 7a, 43100 Parma, Italy

(Received 20 December 2005; accepted 24 April 2006; published online 10 July 2006)

CdTe/CdS/SnO_2/ITO:F solar cell devices were investigated using quantitative secondary ion mass spectrometry (SIMS) depth profiling. They were grown on sapphire substrates and potentially active impurity species were analyzed. The SIMS data were calibrated for both CdS window layer (grown by sputtering) and CdTe absorber layer (deposited by close-space sublimation). For comparison, some of the samples were grown with and without oxygen incorporation into the CdTe layer during its deposition, and with and without postgrowth cadmium chloride ($CdCl_2$) annealing in air and chemical etching. These devices were back contacted using Mo/Sb_2Te_3 sputtered layers. It was shown that for CdTe and CdS layers there was a correlation between the concentrations of oxygen and chlorine. *In situ* oxygen incorporation in the CdTe layer yielded a substantial improvement in the device parameters and achieved an efficiency of 14% compared to 11.5% for devices fabricated in the same conditions without oxygen incorporation in CdTe. In light of our previous reports, this study also led to a clear determination of the origin of Na and Si traces found in these devices.
 [DOI: 10.1063/1.2209788]

I. INTRODUCTION

Increasing the efficiency, reliability, and lifetime of CdTe-based solar cells has been a research focus for the last two decades, and yet the best efficiencies achieved so far are still far below the theoretical limit. In order to reach this goal, surprisingly few of the many approaches have explored the doping of the layers forming the CdTe/CdS junction,[1,2] and led unfortunately to conflicting reports regarding the effect that such doping could have on the performance of the device.[1–3]

$CdCl_2$ is widely used for the heat treatment of the CdTe/CdS device structures, and is also often used as source material providing Cd for the chemical bath deposition of CdS. By using inductively coupled plasma mass spectrometry, we have been able to show that $CdCl_2$ powders supplied by different manufacturers with different nominal purities, already contain substantial amounts of various impurities that have a potential doping effect on both CdTe and CdS.[4] With regard to the impact that the $CdCl_2$ activation process has on CdTe-based solar cells, apparently contradicting reports were published. One found that the Fermi level shifted upwards towards the conduction band following $CdCl_2$ treatment.[5] Another demonstrated that due to an *in situ* $CdCl_2$ treatment, the Fermi level shifts downwards towards the valence band.[6] The latter study also showed that when used *in situ*, this processing step leads to relatively oxide free surface compared to the widely used *ex situ* $CdCl_2$ processing.[6]

In the few reports published so far, secondary ion mass spectrometry (SIMS) was mostly dedicated to the investigation of back contacts and stability of CdTe/CdS solar cells.[7–10] We recently reported a detailed SIMS study of CdTe/CdS/TCO solar cell structures depth profiled throughout using quantitative SIMS from the back and the front side.[11,12] This study exhibited the distribution and concentration of trace elements in the solar cell structures and led to an insight into their main sources.

This investigation is a study of the behavior of CdTe/CdS solar cell devices following an *in situ* oxygen incorporation in the CdTe absorber layer during its growth. We show that oxygen introduction into CdTe increases the performance of these devices by improving all the solar cell parameters. The behavior of impurity species in CdTe and CdS layers, with relevance to these devices, was also carefully looked at using quantitative SIMS depth profiling.

II. EXPERIMENT

Three samples were considered in this study and are summarized in Table I. Our approach was to use sapphire as substrate for its stability at the temperature range used in this

TABLE I. Fabrication conditions of the three CdTe/CdS/TCO/sapphire devices investigated. The effect of oxygen introduction in CdTe is seen for processed device structures by comparing samples 85 and 89, while comparison of samples 87 and 89 shows the effect of $CdCl_2$ treatment and the subsequent chemical etching when the CdTe layer is grown with oxygen incorporated in it.

Sample number	Introduction of O in the CdTe layer during growth	$CdCl_2$ treatment and subsequent Br_2-methanol etching
85	No	Yes
87	Yes	No
89	Yes	Yes

[a]Present address: Clarendon Laboratory, Department of Physics, University of Oxford, Parks Road, Oxford, OX1 3PU, United Kingdom; electronic mail: m.emziane1@physics.oxford.ac.uk

TABLE II. Summary of SIMS measurement conditions and relative sensitivity factors (RSFs) used for CdS and CdTe.

Isotope profiled	Primary beam	CdS matrix	CdTe matrix	CdS RSFs	CdTe RSFs
18O	Cs	34S	122Te	4.36×10^{23}	8.78×10^{22}
19F	Cs	34S	122Te	7.00×10^{19}	3.50×10^{19}
23Na	O	34S	122Te	3.21×10^{16}	5.42×10^{16}
28Si	O	34S	122Te	2.97×10^{19}	1.97×10^{20}
34S	Cs	34S	122Te	2.42×10^{21}	2.42×10^{21}
37Cl	Cs	34S	122Te	2.75×10^{20}	1.18×10^{20}
81Br	Cs	34S	122Te	1.12×10^{20}	5.60×10^{19}
115In	O	34S	122Te	6.86×10^{17}	1.64×10^{17}
118Sn	O	34S	122Te	2.97×10^{19}	1.50×10^{18}

investigation, therefore avoiding the diffusion into the structures of impurity elements from the more widely used glass substrates.[11,12] Prior to the structure deposition, 25 $\times$25 mm^2 and 0.5-mm-thick sapphire substrates were thoroughly cleaned with ethanol, ammonia, acetone, and isopropyl alcohol. The transparent conducting oxide (TCO) bilayer consisted of a fluorine doped indium tin oxide (ITO:F) film ($\sim$1.2 μm thick) followed by a tin oxide (SnO_2) film of about 300 nm thickness. It was deposited by reactive sputtering at a substrate temperature around 450 °C, an $Ar+O_2$ atmosphere was used for both layers while CHF_3 was added in the case of ITO:F. The $\sim$80-nm-thick CdS:F layer was then deposited by reactive sputtering in a different chamber using Ar and CHF_3 flows at a substrate temperature of 200 °C and a total pressure of 5×10^{-3} mbar. Finally, the deposition of the $\sim$8-μm-thick CdTe layer was performed by close space sublimation (CSS) where the source temperature was kept at 750 °C while the substrate temperature was in the range of 480–540 °C. The distance source substrate was 2–3 mm. Oxygen was intentionally introduced *in situ* by letting O_2 into the CSS chamber during the deposition of the CdTe layers for two of the devices. The total pressure (Ar and O_2) was 100 mbars with 5 mbars O_2 partial pressure. The CdTe layer of the remaining device was grown under the same conditions but without oxygen. Two of the samples (85 and 89) then underwent a $CdCl_2$ processing via thermal evaporation of $CdCl_2$ powder on top of the structures and air annealing (400 °C for 30 min), followed by a chemical etching in bromine-methanol solution. The purity of the starting materials used in this study was 6, 4, and 3*N* for CdTe, CdS, and $CdCl_2$, respectively. The sapphire substrates used had 5*N* purity. The back contact consisted of sputtered Sb_2Te_3 and Mo layers deposited at 300 °C and room temperature, respectively.

The devices were investigated using quantitative SIMS depth profiling (Cameca IMS 4f, QinetiQ UK). O and Cs primary ion beams were rastered over an area of 175 μm diameter to profile Si, In, Cl, Na, O, Sn, F, Br, and S. The secondary ions were collected from the center of the craters through a circular area of 60 and 33 μm diameter, for O and Cs, respectively. 5*N* purity CdTe and CdS single crystals were used to implant the species studied in order to obtain their relative sensitivity factors (RSFs) necessary for the SIMS quantification, except for F and Br where the RSFs were extrapolated from HgCdTe implants. The RSF values used and other conditions of SIMS measurements are summarized in Table II. Device characteristics were measured under standard conditions (AM 1.5 and a light power of 100 mW/cm^2) in order to determine the device parameters.

III. RESULTS AND DISCUSSION

We will focus on the effect of oxygen incorporation in CdTe combined with the residual contaminants present in $CdCl_2$ that are relevant to CdTe-based solar cell devices through their effect on the optoelectrical properties of CdTe and CdS layers of the structures. The quantitative SIMS data for the CdTe and CdS layers will be presented and discussed separately in Secs. III A and III B.

A. Impurity species in the CdTe absorber layer

In this section, the presence and distribution of impurities in the CdTe layer of the devices will be looked at. For this purpose, all the SIMS data shown in this section were calibrated using exclusively CdTe RSFs, meaning that they are quantitative for CdTe but only qualitative for the CdS window layer.

Figure 1 shows O and Cl depth profiles throughout the structures of the three samples. The highest oxygen concentration was found in the CdTe layer when its growth was performed with O_2 incorporation. This can be seen in Fig. 1 by comparing samples 85 and 89, both of which were $CdCl_2$-treated. A comparison between samples 87 and 89 leads also to an interesting conclusion which is that the concentration of oxygen in CdTe is further increased when the sample receives a postgrowth heat treatment in $CdCl_2$ (sample 89) as compared to the sample without $CdCl_2$ treatment (sample 87), although the CdTe layer of both samples was grown in presence of oxygen.

With regard to chlorine content in CdTe, it appears that this is about two orders of magnitude higher for $CdCl_2$-treated samples (85 and 89) versus the untreated one (87). Moreover, for the two treated samples, the Cl concentration is even higher when the sample already contains oxygen in CdTe following its introduction during the growth (sample 89 versus sample 85). It turns out therefore that the

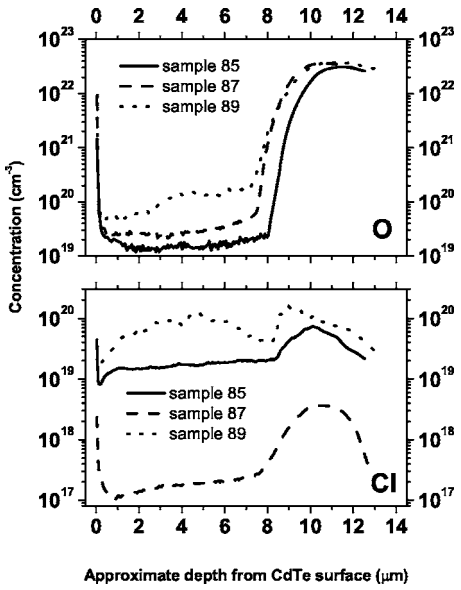

FIG. 1. SIMS depth profiles of Cl and O in CdTe/CdS/SnO_2/ITO:F solar cell devices grown on sapphire substrates. The calibration was done according to RSFs in CdTe layer. Only samples 87 and 89 were grown with oxygen incorporated in their CdTe layer during its growth, and only samples 85 and 89 underwent a postgrowth processing (Table I).

amounts of Cl and O in the CdTe layer are somehow interdependent, i.e., the presence of one of them favors the presence of the other.

Figure 2 shows Br, F, In, Sn, Na, and Si depth profiles in all three samples. Bromine shows similar diffusionlike profiles for both processed samples (85 and 89) with a steadily increasing concentration from the CdTe/CdS interface to the CdTe surface. This is in contrast with the Br profile from the unprocessed sample (87) that is flat throughout CdTe with a concentration of 5×10^{19} cm^{-3}, and confirms that Br presence in CdTe is due to the bromine-methanol chemical etching performed on the processed samples following the $CdCl_2$ heat treatment and prior to the back contact deposition. Fluorine has a constant concentration within the CdTe layer for the processed samples, but in the unprocessed sample the profile is not flat in CdTe, meaning that F profile flattens upon heat treatment. The depth profiles shown by indium and tin are flat with concentrations in CdTe in the range of 5×10^{14}–10^{15} cm^{-3} for In and 10^{14} cm^{-3} for Sn regardless of the sample preparation conditions except for In in sample 89 where some increase is seen at a depth between 3 and 7 μm within CdTe. Sodium profiles are flat in CdTe for samples 85 and 89 and more spread out in sample 87 but with concentrations of 5×10^{16} cm^{-3} for the $CdCl_2$-treated samples (85 and 89) and only 10^{15} cm^{-3} for the sample that did not receive any treatment with $CdCl_2$ (87). This indicates therefore that the increase in Na concentration in CdTe following $CdCl_2$ treatment is a direct consequence of the Na already present in the $CdCl_2$ powder used for the treatment, as carefully checked in our separate study.[4] This is also corroborated by comparing the Na concentration measured in CdTe layer of samples grown on soda-lime glass substrates and shows clearly that Na is exclusively due to $CdCl_2$ in this particular case where sapphire substrates were used.[11] Within the accuracy of this SIMS analysis, the incorporation of oxygen in CdTe was not found to have any particular effect on the distribution or concentration of Na, Br, F, In, and Sn.

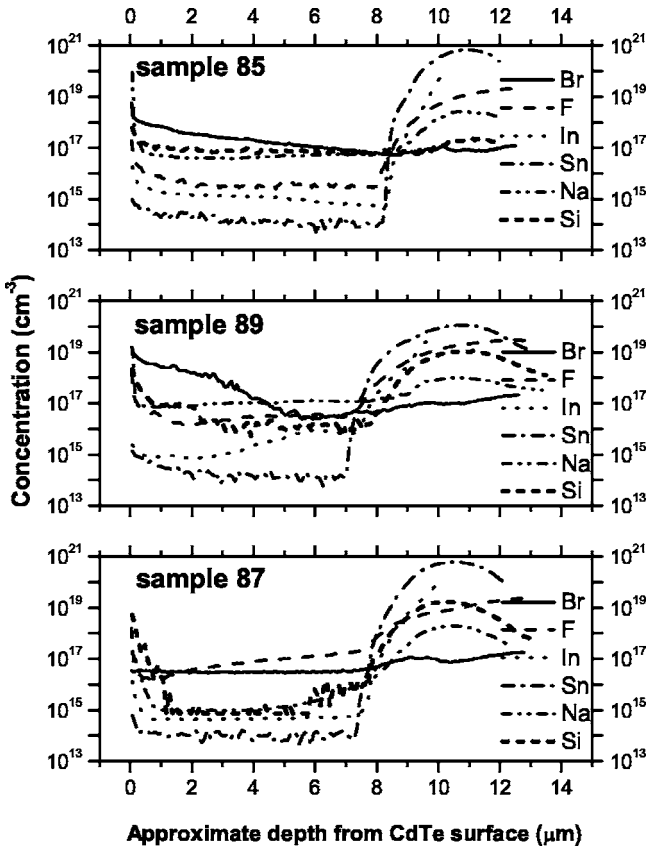

FIG. 2. SIMS depth profiles of Br, F, In, Sn, Na, and Si in CdTe/CdS/SnO_2/ITO:F solar cell devices grown on sapphire substrates. The calibration was done according to RSFs in CdTe layer. Only samples 87 and 89 were grown with oxygen incorporated in their CdTe layer during its growth, and only samples 85 and 89 underwent a postgrowth processing (Table I).

Silicon concentration in CdTe decreases from $\sim10^{17}$ cm^{-3} in sample 85 to $\sim10^{16}$ cm^{-3} in sample 89 to below $\sim10^{15}$ cm^{-3} in sample 87, i.e., below the detection limit of the SIMS system used. This suggests that the presence of oxygen in CdTe (samples 87 and 89) tends to lower the content of Si and it is lowered further when the sample does not receive any $CdCl_2$ treatment or chemical etching (sample 87). It should be recalled here that, as detailed in our reported study,[4] no trace of Si was detected in the $CdCl_2$ powder used for the treatment of these samples. This also excludes the possibility of Si migration from the substrate as suggested in our previous study of device structures grown on soda-lime glass since sapphire was used here as substrate.[11] One can therefore only suspect a Si contamination during the chemical etching process that is performed in a borosilicate glass beaker with the same etching solution used to etch several samples most of them were grown on soda-lime glass substrates. This plausible origin of Si is emphasized by the gradient shown by Si in the first ~3 μm from the CdTe surface downwards in the etched samples (85 and 89) compared to the unetched one (87). It is also supported by the fact that for the samples grown on soda-lime glass substrates, the increase in the Si concentration is also

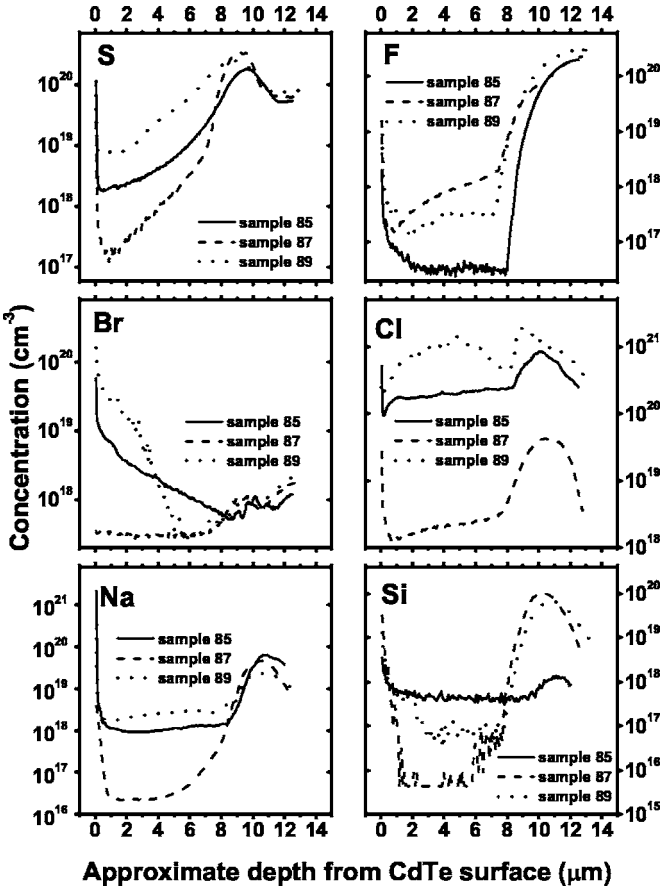

FIG. 3. SIMS depth profiles of S, F, Br, Cl, Na, and Si in CdTe/CdS/SnO_2/ITO:F solar cell devices grown on sapphire substrates. The calibration was done according to RSFs in CdS layer except for S where the concentration is in arbitrary units. Only samples 87 and 89 were grown with oxygen incorporated in their CdTe layer during its growth, and only samples 85 and 89 underwent a postgrowth processing as shown in Table I.

about one order of magnitude (from 3×10^{15} to 4×10^{16} cm^{-3}) for the etched samples versus the unetched ones.[11]

The layer depth scales shown in Figs. 1 and 2 were calibrated according to the sputter rate in CdTe. This allowed determination of the thickness for the CdTe layers: sample 85 has the thickest CdTe layer ($\sim$8.5 μm) while samples 87 and 89 have CdTe thicknesses of about 7.5 μm.

B. Impurity species in the CdS window layer

Since the CdS layer is comparatively very thin, it has not been possible to resolve all the impurity species investigated in this study in the CdS. We will therefore show only the depth profiles for which the CdS layer was resolved, as no quantitative information could be extracted from the remaining profiles where it was very hard to distinguish signals in the CdS from tails in the CdTe and TCO layers.

Figure 3 shows the depth profiles of F, Br, Cl, Na, and Si quantified using CdS RSFs. S profiles, with concentrations in arbitrary units, were added in this figure to provide an approximate determination of the location and extent of the CdS layer within the structures. However, an accurate quantification of the depth profiled is complicated by changes in sputter rate at different interfaces. As mentioned in the previous section, the layer depth scales were calibrated according to the sputter rate in CdTe that is larger than in CdS, leading to a CdS layer that appears much broader than its nominal thickness. The CdS layer appears thicker also because of the initial roughening of the CdTe surface as exhibited by the shape of most of the profiles near this surface, i.e., in the SIMS transient region.

For fluorine, CdS layer can only be slightly resolved for sample 87 (untreated) with a maximum concentration shoulder around 5×10^{19} cm^{-3} but for both treated samples 85 and 89, F is found to interdiffuse at the CdS/TCO interface to the extent that its profiles do not resolve the CdS layer. Bromine has a peak concentration in CdS of about 10^{18} cm^{-3} for all three samples. However, like F, Br peak in CdS is better resolved for the untreated sample than for the treated ones. Also, both F and Br in CdS do not seem to have any correlation with the oxygen concentration in CdTe. Chlorine has a similar behavior in CdS as seen above for CdTe. Indeed, the treated samples have a Cl concentration in CdS $[(1-2)\times10^{21}$ cm$^{-3}]$ up to 200 times higher compared to the untreated one (4×10^{19} cm^{-3}). Furthermore, when oxygen is incorporated in CdTe, it leads also to a two times increase in the Cl concentration in CdS as if there is an interdependence between O (in CdTe) and Cl in terms of presence and concentration. Na profiles show a peak in the CdS layer with a concentration that does not seem to depend either on the $CdCl_2$ treatment or the oxygen incorporation during CdTe deposition—the peak concentration is $\sim5\times10^{19}$ cm^{-3} for both samples 85 and 87. Unlike its behavior in CdTe, the Si peak concentration in CdS decreases from 10^{20} cm^{-3} before $CdCl_2$ treatment to 6×10^{19} cm^{-3} and 10^{18} cm^{-3} upon treatment, respectively, for samples grown with and without oxygen. Si behavior in CdS is, however, in agreement with our findings for CdS layers of device structures depth profiled from the front side and was interpreted by the possible formation of $SiCl_4$ compound that is gaseous at the heat treatment temperature used.[12]

The oxygen profile could not be resolved in the CdS layer and therefore the oxygen concentration in CdS could not be measured and compared for the devices considered. As a result, no conclusion could be made as to whether the intentional introduction of oxygen in CdTe during its growth enhances the oxygen concentration in CdS although the oxygen presence in CdTe was found to increase the chlorine concentration in CdS as shown above. Overall, from S profiles shown in Fig. 3, CdS layer seems to have sharper interfaces for sample 87 (untreated) and interdiffused and thus broader ones for the treated samples (85 and 89), especially the interface with the CdTe layer.

C. On the resulting solar cell devices

It should be noticed that the back contact deposition together with the device assessment were carried out after SIMS measurements were completed. About five months elapsed between the initial growth of these structures and the final measurements of their device characteristics.

The device made from sample 87 did not give any result since there were many pinholes in the layers. The current-

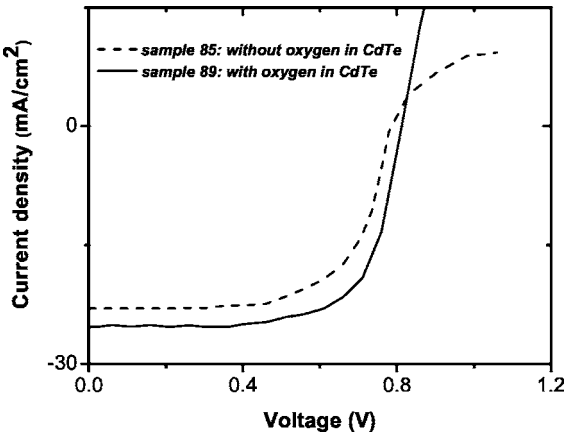

FIG. 4. Current vs voltage (*I-V*) curves of samples 85 and 89.

voltage (*I-V*) characteristics measured for samples 85 and 89 are shown in Fig. 4. The device parameters of 1 cm^2 solar cell from samples 85 and 89 were reported recently and it was found that the device parameters of sample 89 (with O in CdTe) were all increased compared to those of sample 85 (without O in CdTe).[13] This relative increase was ~4% for the open-circuit voltage (from 780 to 812 mV), ~9% for the short-circuit current density (from 23 to 25 mA/cm^2) and ~8% for the fill factor (from 0.64 to 0.69). The device efficiency increased from 11.5% for sample 85 to 14% for sample 89, i.e., an improvement of ~22% as a result of O introduction in CdTe.[13]

It is believed that *in situ* oxygen incorporation into CdTe together with the increased concentration of chlorine in CdTe and in CdS due to this presence of oxygen may both contribute to the improvement of the solar device parameters. O and consequently Cl seem therefore to be electrically active and/or form electrically active complexes within the CdTe absorber layer and, to a less extent, within the CdS window layer as well, leading ultimately to an improved overall performance of the CdTe/CdS solar cell device.

IV. CONCLUSION

CdTe/CdS photovoltaic devices were fabricated on sapphire substrates using SnO_2/ITO:F as TCO bilayer and Mo/Sb_2Te_3 as back contact. The CdTe layer was deposited with oxygen introduction during its growth and the device structures were postdeposition heat treated with $CdCl_2$ and chemically etched.

We found that an intentional *in situ* introduction of oxygen into the CdTe absorber layer affected the resulting device by improving all its parameters, and led to an enhanced efficiency of 14% compared to 11.5% for devices fabricated in the same conditions without oxygen incorporation in CdTe during its growth.

Quantitative SIMS investigation was carried out on the devices and revealed that oxygen and chlorine were interdependent in terms of presence and concentration separately in CdTe as well as in CdS to a lesser extent. In other words, oxygen incorporation in CdTe layer was found to favor the uptake of Cl in both CdTe and CdS layers. The increased Na concentration in CdTe was found to be caused solely by the $CdCl_2$ treatment and Na concentration in CdS was unchanged. Br was found to originate from the chemical etching and F profile was shown to flatten following processing. Si was found to behave differently in CdS and CdTe while Cl had a similar behavior in both layers. The presence of oxygen had no observable effect on Br, F, In, and Sn in either CdTe or CdS.

ACKNOWLEDGMENTS

The authors are thankful to the EPSRC for financial support under Grant No. GR/R39283/01, and to A. J. Pidduck and A. J. Simons (QinetiQ, UK) for SIMS measurements.

[1] T. Chandra and S. Bhushan, J. Phys. D **37**, 2945 (2004), and references therein.
[2] D. S. Boyle, S. Hearne, D. R. Johnson, and P. O'Brien, J. Mater. Chem. **9**, 879 (1999).
[3] M. Altosaar, K. Ernits, M. Danilson, J. Krustok, L. Kaupmees, T. Varema, J. Raudoja, and E. Mellikov, Thin Solid Films **480–481**, 147 (2005).
[4] M. Emziane, C. J. Ottley, K. Durose, and D. P. Halliday, J. Phys. D **37**, 2962 (2004).
[5] T. Schulmeyer, J. Fritsche, A. Thißen, A. Klein, W. Jaegermann, M. Campo, and J. Beier, Thin Solid Films **431–432**, 84 (2003).
[6] K. Vamsi Krishna and V. Dutta, J. Appl. Phys. **96**, 3962 (2004).
[7] D. L. Batzner, A. Romeo, M. Terheggen, M. Dobeli, H. Zogg, and A. N. Tiwari, Thin Solid Films **451–452**, 536 (2004).
[8] K. D. Dobson, I. Visoly-Fisher, G. Hodes, and D. Cahen, Adv. Mater. (Weinheim, Ger.) **13**, 1495 (2001).
[9] K. D. Dobson, I. Visoly-Fisher, G. Hodes, and D. Cahen, Sol. Energy Mater. Sol. Cells **62**, 295 (2000).
[10] C. Narayanswamy, T. A. Gessert, and S. E. Asher, AIP Conf. Proc. **462**, 248 (1999).
[11] M. Emziane, K. Durose, N. Romeo, A. Bosio, and D. P. Halliday, Semicond. Sci. Technol. **20**, 434 (2005).
[12] M. Emziane, K. Durose, D. P. Halliday, N. Romeo, and A. Bosio, J. Appl. Phys. **97**, 114910 (2005).
[13] M. Emziane, K. Durose, D. P. Halliday, A. Bosio, and N. Romeo, Appl. Phys. Lett. **87**, 261901 (2005).